International Journal of Applied Mathematics
Volume 36 No. 2 2023,
ISSN: 1311-1728 (printed version); ISSN: 1314-8060 (on-line version)

SIMULATION OF THREE-DIMENSIONAL UNSTEADY MHD NANOFLUID FLOW OVER A PERMEABLE ROTATING EXPANDING DISK WITH CONVECTIVE BOUNDARY INFLUENCE

Tapas Datta[1], Arindam Das[2], Arijit Mandal[3]

[1]Department of Mathematics, Aghore Kamini Prakash Chandra Mahavidyalaya, Bengai, Hooghly, West Bengal - 712611

[2]Assistant Teacher of Mathematics, Bhubanmayee Jr. High School, Pandapara Kalibari, Jalpaiguri,735132, West Bengal, India

[3]Assistant Teacher, Buridaha Primary School, Buridaha, Dighalbar, Gazole, Malda, West Bengal -732138

Abstract: Here we are going to research heat and mass exchange capacity of unsteady Magneto hydrodynamic nanofluid stream streaming over a porous spinning and rotating disk. Different convective conditions are mulled over at the limit of the stream. The usage of similarity transformation has been considered to change over the suit of partial differential equations in the numerical model portraying the stream into a bunch of ordinary differential equations alongside the appropriate boundary conditions. The authors considered the revolution and extending of the disk and portrayed the outcomes acquired in two conditions like extending and no extending disk through proper graphs. After the exhausting examination of the stream it is discovered that the presence of expanding plate lifts the impacts of heat convection factor, nanoparticle volume fraction convection factor, Prandtl number and stretching disk factor on the heat and mass exchange qualities of the stream proficiently. As needs be, the heat and mass exchange pace of the stream at the stream surface are essentially expanded in presence of suction and no suction in the flow.

Keywords: Unsteady; Nanofluid Flow; Expanding disk; rotating disk; multiple convective boundary conditions.

2010 MATHEMATICS SUBJECT CLASSIFICATION: 76W05

1. INTRODUCTION:

Nanofluids are created by scattering the nanometer-scale strong particles into base fluids with low thermal conductivity, for example, water, ethylene glycol, oils, and so forth Control of heat move in numerous energy frameworks is critical in view of the expansion in energy costs. Lately, nanofluids innovation is proposed and concentrated by certain scientists tentatively or mathematically to control heat move in a cycle. The nanofluid can be applied to designing issues, for example, heat exchangers, cooling of electronic hardware, and compound

Received: April 10, 2023

ISSN: 1311-1728 (printed version); ISSN: 1314-8060 (on-line version)

cycles. There are two different ways for recreation of nanofluid: single stage and two stages. In the main technique, specialists expected that nanofluids are treated as the regular unadulterated liquid and ordinary conditions of mass, force, and energy are utilized and the solitary impact of nanofluid is its warm conductivity and consistency, which are acquired from the hypothetical models or test information. These analysts accepted that nanoparticles are in warm harmony and there are no slip speeds between the nanoparticles and liquid particles; accordingly, they have a uniform combination of nanoparticles. In the subsequent technique, scientists expected that there are slip speeds among nanoparticles and liquid particles. So the volume division of nanofluids may not be uniform any longer and there would be a variable centralization of nanoparticles in a blend. There are a few mathematical and semi logical strategies that have been utilized by a few creators to reproduce nanofluid stream and heat move. The primary point behind the presentation of 'Nanofluid' was to expand the warm stream limit of the liquid with the assistance of metallic, non metallic nanoparticles. Choi [01] was the first to acquaint the ideas of nanofluids with the world. At that point a few specialists persistently attempted to set up the productivity of nanofluid in the field of medication conveyance, nano central processor creation, front line batteries creation, energy effective heat exchangers, sun powered energy creations and so forth Others were attempting to discover overhauled hypothetical stream models to best portray the stream circumstances in numerous modern creations. To examine the warm properties of the base liquid, Buongiorno [02] proposed a numerical model utilizing the thermophoresis and Brownain movement effects on improve the warm properties in base liquid. He found that the traditional liquid with thermophoresis and Brownain movement assumes a huge part in improving the liquid's warm conductivity. The investigation of polarized three-dimensional progression of nanofluid with nonlinear warm radiation is examined by Hayat et al. [03].

I V Shevchuk [4] presented consequences of the analytical and mathematical displaying of convective heat and mass exchange in various pivoting streams brought about by (I) framework revolution, (ii) twirl streams because of whirl generators, and (iii) surface arch reciprocally and curves. The current examination is engaged to additionally expand the thick siphoning issue given by [5] for Maxwell liquid model over a turning plate with extra consideration of the effect of disk vertically upward/descending development. Taking into account the spearheading examination of von Karman in 1921, various actual frameworks have been demonstrated and dissected to the regular turning disk stream issues. For brevity, a portion of these issues are given in current examination. For example, Millsaps and Pohlhausen [6] inspected the uniform pull sway on the progression of pivoting disk. It was seen that the greatness of the outspread stream part reduces rapidly with the development of attractions boundary. The heat move because of plate revolution was examined in early examinations see Refs. [7-8]. Right when the stream was started indiscreetly from rest was inspected by Benton [9]. The acquired actual issue was handled mathematically. Kuiken [10] characterized the outcomes about the effect of blowing because of penetrable turning plate. Watson and Wang [11] spoke to the effect of rotational deceleration. Tooth and Tao [12] further added such enhancements when the rotational plate was radially extended. The assurance of the Karman

ISSN: 1311-1728 (printed version); ISSN: 1314-8060 (on-line version)

answer for the turning plate was accounted by Turkyilmazoglu and Uygun [13]. The gooey liquid in a pivoting plate of an incompressible stream, where the disk divider bears slip impacts, was accounted for by Miclavcic and Wang [14]. A comparable report was drawn out toward the magneto hydrodynamic impacts as announced by Turkyilmazoglu [15]. Moreover, Turkyilmazoglu [16] incorporated the impacts of plate surface. Bachok et al. [17] examined the consistent incompressible gooey nanofluid because of a turning plate. They settled it mathematically by a limited distinction conspire, in particular the Keller-box technique, considering two models for the successful warm conductivity of the nanofluid, to be specific the Maxwell–Garnett model and the Patel model. They inferred that the warmth move rate expanded with the estimations of nanoparticle volume part lead to an abatement in the warmth move rate at the surface for pull, however increments for infusion for both model. Different sorts of the nanoparticles inside the pivoting plate stream were incorporated, and their mathematical assessment was completed by Turkyilmazoglu [18]. The investigation of micropolar liquid in MHD stream over a turning disk was expressed by Doh and Muthtamilselvan [19]. The Reiner–Rivlin liquid model in a turning disk stream was given by Tabassum and Mustafa [20]. Moreover, the direct mathematical reproduction of fierce pivoting profile is given by Appelquist et al. [21].

For all intents and purposes, when there exist a temperature contrast among surface and liquid, at that point the convective heat transport component can't be ignored. That is the reason in various innovative and designing fields convective limit condition plays out a crucial job in the heat transport component [22]. Essentially, Convective mass vehicle assigns a system through which travel of mass is happened between the strong surface and the liquid, because of the engendering of mass or matter from the strong to liquid. It might likewise be seen between two immiscible liquid withdrew by a versatile interface. It is the joint mix of dispersion for example irregular development of atoms and shift in weather conditions for example mass movement of particles conveyed by moving liquid. To build up a more productive and ideal counterfeit kidney, numerous exploratory methodologies have been utilized to examine mass exchange inside, outside, and cross empty fiber films with various types of layers, solutes, and stream rates as boundaries. Notwithstanding, these trial approaches are costly and tedious. Mathematical figuring and PC reenactment is a powerful method to contemplate mass exchange in the counterfeit kidney, which can save considerable time and diminish trial cost. Liao et al. [23] presents another model to reproduce mass exchange in fake kidney by coupling together shell-side, lumen-side, and trans film streams. Kooijman and Taylor [24] featured irregularities in the displaying of mass exchange in multi segment refining segments. Models of stream and mass exchange are built up that look to keep away from these irregularities dependent on the standard suspicions of attachment stream of fume and of fitting stream or pivotal scattering of the fluid. Saif et al. [25] investigated Darcy–Forchheimer stream of thick nanofluid by bended stretchable surface. Stream in permeable medium is portrayed by Darcy–Forchheimer connection. Brownian dissemination and thermophoresis were thought of. Convective warmth and mass limit conditions were likewise utilized at the bended stretchable surface. Mehmood et al. [26] mathematically researched limit layer stream of nanofluid over a twisted extending surface. They completed their examination by considering convective mass transition condition. Commitment of gooey dispersal is considered alongside warm radiation. Results denoted that temperature, fixation turns into an expanding capacity of bend boundary. Impacts of convective heat and mass vehicle on nanofluid stream over nonlinear bended surface were tended to by Hayat et al. [27]. Results passed on that heat and mass vehicle drop off for thermophoresis. Convective Jeffry liquid stream because of the bended surface was dissected by Imtiaz et al. [28]. A homogeneous–heterogeneous responsive instrument was incorporated by them. Results investigated that warm Biot number improve the temperature and heat transport. An examination investigating the impact of second-order slip instrument on nanofluid stream disregarding a penetrable extending surface was researched by Acharya et al. [29]. Also they had caught the stream highlights including the presence of sensible warm and solutal limit conditions. The impression of multiple convective conditions on Falkner-Skan stream along a penetrable static/moving wedge is exhibited by Chakrobarty et al. [30]. They actualized Carreau nanofluid model contingent upon the force law file with the impacts of thermophoresis and Brownian movement. They discovered that with the improvement of Brownian movement boundary, the pace of warmth transport gets decreased for static wedge by 14.25% while for moving wedge the decrease is 10.61%. Another critical perception shows that the development in mass vehicle with conduction dispersion is 17.65% more noteworthy for moving wedge rather than static one as per other administering boundaries.

Since there is no work done involving multiple convective boundary conditions in the nanofluid flow over expanding and spinning disk, we are intended to do the analysis. Our Aim is to analyze the effects of multiple convective factor, Prandtl Number and stretching factor on the heat and mass transfer capacity of the flow system. We compare our findings in two different cases where suction and no suction of the disk are taken into consideration.

2. MATHEMATICAL MODELING:

An unsteady, incompressible 3D MHD boundary layer flow of nanofluid over a permeable disk is modeled here. The flow is assumed to be generated by a rotating and stretching of the disk. All physical quantities are not depending on ϕ, as the flow is axis-symmetric about z direction. The stagnation point is at the surface ($z=0$) and the fluid streams at ($z\geq 0$) the upper half plane as appeared in figure 1.

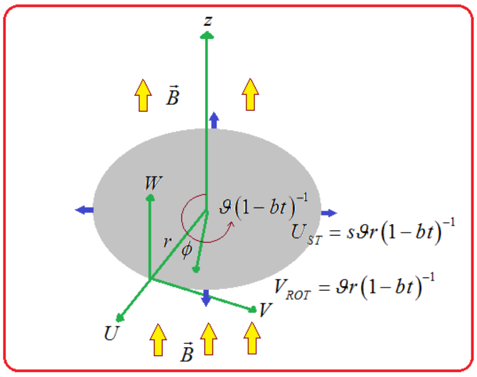

FIGURE 1: PHYSICAL MODEL OF THE FLOW

International Journal of Applied Mathematics

Volume 36 No. 2 2023,

ISSN: 1311-1728 (printed version); ISSN: 1314-8060 (on-line version)

The disk at $z=0$ is rotated by uniform angular velocity $\vartheta(1-bt)^{-1}$. Here, the magnetic field $\vec{B}$ acts in the vertical direction. The disk is assumed porous with mass flux velocity W_{SUC}. The Buongiorno's model for nanofluid is used to discuss the thermophoresis and Brownian motion due to nanoparticles. The surface of the disk is heated by the convection from the hot fluid of temperature $T_{BD}\,(>T_\infty)$, which provides a heat transfer coefficient C_{HT}. Subsequently, the thermal convective boundary condition generates. Similarly, the concentration of the disk $N_{BD}\,(>N_\infty)$ provides a mass transfer coefficient C_{MT}. In the following mathematical formulation, we have denied the presence of viscous dissipation, joule heating, thermal slip, and chemically reactive flow. Under the above-stated conditions, the governing equations for the given non-linear problem are

$$\left.\begin{aligned}
&\frac{\partial U}{\partial r}+\frac{U}{r}+\frac{\partial W}{\partial z}=0\\
&\frac{\partial U}{\partial t}+U\frac{\partial U}{\partial r}+W\frac{\partial U}{\partial z}-\frac{V^2}{r}=\nu\frac{\partial^2 U}{\partial z^2}-\frac{\nu U}{K_1}-\frac{\sigma B^2 U}{\rho}\\
&\frac{\partial V}{\partial t}+U\frac{\partial V}{\partial r}+W\frac{\partial V}{\partial z}+\frac{UV}{r}=\nu\frac{\partial^2 V}{\partial z^2}-\frac{\nu V}{K_1}-\frac{\sigma B^2 V}{\rho}\\
&\frac{\partial T}{\partial t}+U\frac{\partial T}{\partial r}+W\frac{\partial T}{\partial z}=\alpha\frac{\partial^2 T}{\partial z^2}+\tau\left(D_B\frac{\partial T}{\partial z}\frac{\partial N}{\partial z}+\frac{D_t}{T_\infty}\left(\frac{\partial T}{\partial z}\right)^2\right)\\
&\frac{\partial N}{\partial t}+U\frac{\partial N}{\partial r}+W\frac{\partial N}{\partial z}=D_B\frac{\partial^2 N}{\partial z^2}+\frac{D_t}{T_\infty}\frac{\partial^2 T}{\partial z^2}
\end{aligned}\right\}$$

(1)

And the boundary conditions are

$$\left.\begin{aligned}
&U=U_{ST}=\frac{s\vartheta r}{1-bt},V=V_{ROT}=\frac{\vartheta r}{1-bt},W=W_{SUC},-\kappa\frac{\partial T}{\partial z}=C_{HT}\left(T_{BD}-T\right),-D_B\frac{\partial N}{\partial z}=C_{MT}\left(N_{BD}-N\right)\text{ at z}=0\\
&U\to 0,V\to 0,W\to 0,T\to T_\infty,N\to N_\infty\text{ as z}\to\infty
\end{aligned}\right\}$$

(2)

Here (U,V,W) are the velocity components of the flow in radial, tangential and z-direction respectively, ν is kinematic viscosity, K_1 is porosity of the disk, α is thermal intake capacity of the fluid, τ is the ratio of specific heat of the nanofluid and nanoparticle, D_B is Brownian motion factor, D_t is thermophoresis factor.

Since the suit of pdes in equations (1) along with boundary conditions (2) are highly nonlinear, so to solve the problem, we need to transform equations (1) with (2) into suit of odes. To achieve this we apply the dimensionless similarity transformations given below

$$\zeta=\sqrt{\frac{\vartheta}{\nu}}\frac{z}{\sqrt{1-bt}},U=\frac{\vartheta r}{1-bt}f'(\zeta),\mathrm{V}=\frac{\vartheta r}{1-bt}g(\zeta),W=\frac{-2\sqrt{\vartheta\nu}}{\sqrt{1-bt}}f(\zeta),\chi=\frac{T-T_\infty}{T_{BD}-T_\infty},\varphi=\frac{N-N_\infty}{N_{BD}-N_\infty}$$

(3)

ISSN: 1311-1728 (printed version); ISSN: 1314-8060 (on-line version)

After the application of the similarity transformations the equation (1) along with boundary conditions (2) transforms into the following set of odes

$$\left.\begin{aligned} & f''' + 2ff'' - f'^2 + g^2 - S_{utd}\left(f' + \frac{1}{2}\zeta f''\right) - (M+K)f' = 0 \\ & g'' + 2(g'f - gf') - S_{utd}\left(g + \frac{1}{2}\zeta g'\right) - (M+K)g = 0 \\ & \chi'' + N_B\chi'\varphi' + N_t(\chi')^2 + Pr\left(2f\chi' - \frac{1}{2}S_{utd}\zeta\chi'\right) = 0 \\ & \varphi'' + \frac{N_t}{N_B}\chi'' + Le.Pr\left(2f\varphi' - \frac{1}{2}S_{utd}\zeta\varphi'\right) = 0 \end{aligned}\right\}$$

(4)

And the converted boundary conditions are

$$\left.\begin{aligned} & f(0)=\lambda, g(0)=1, f'(0)=s, \chi'(0)=-Bi_t(1-\chi(0)), \varphi'(0)=-Bi_c(1-\varphi(0)) \\ & f(\infty)=0, g(\infty)=0, f'(\infty)=0, \chi(\infty)=0, \varphi(\infty)=0 \end{aligned}\right\}$$

(5)

Here $S_{utd} = b\vartheta^{-1}$ unsteady factor, $M = \sigma B^2(1-bt)(\vartheta\rho)^{-1}$ reduced magnetic parameter, $K = \nu(1-bt)(\vartheta K_1)^{-1}$ porosity parameter, $N_B = \tau D_B \alpha^{-1}(N_{BD} - N_\infty)$ dimensionless Brownian parameter, $N_t = \tau D_t(\alpha T_\infty)^{-1}(T_{BD} - T_\infty)$ reduced thermophoresis parameter, $Pr = \nu\alpha^{-1}$ Prandtl number, $Le = \alpha D_B^{-1}$ Lewis number, s is expanding parameter, $\lambda = -W_{SUC}(1-bt)^{0.5}(4\vartheta\nu)^{-0.5}$ suction injection parameter, $Bi_t = C_{HT}\kappa^{-1}\sqrt{\nu(1-bt)\vartheta^{-1}}$ thermal Biot number, and $Bi_c = C_{MT}D_B^{-1}\sqrt{\nu(1-bt)\vartheta^{-1}}$ mass Biot number.

The thermal flow rate at the surface is $q_w = -\kappa\left(\frac{\partial T}{\partial z}\right)_{z=0}$ and the mass flow rate at the disk is $q_m = -D_B\left(\frac{\partial N}{\partial z}\right)_{z=0}$. So the Nusselt number is described as $Nu = \frac{rq_w}{\kappa(T_{BD} - T_\infty)}$ and the Sherwood number can be formulated as $Sh = \frac{rq_m}{D_B(N_{BD} - N_\infty)}$. Then the reduced Nusselt number and Sherwood number take the shape as $Nu_r = (Re_r)^{-0.5}(1-bt)^{0.5}\,Nu = -\chi'(0)$ and $Sh_r = (Re_r)^{-0.5}(1-bt)^{0.5}\,Sh = -\varphi'(0)$ where $Re_r = \frac{\vartheta r^2}{\nu}$ local Reynolds number.

3. SOLUTION PROCESS:

The arrangement of ordinary differential equations in (4) alongside decreased limit conditions (5) is non-linear in nature. We use Boundary Value Problem Midrich plot for dealing with the non-straight differential equations. The arrangements of the stream issue are created by using Maple17 programming. The overall technique for the methodology is portrayed by

$$\omega'(\theta) = F(\theta, \omega(\theta)), \omega(\theta_0) = \omega_0 \tag{6}$$

International Journal of Applied Mathematics
Volume 36 No. 2 2023,
ISSN: 1311-1728 (printed version); ISSN: 1314-8060 (on-line version)

The term used for the modified Euler method is

$$\omega_{n+1} = \omega_n + h^* F\left(\theta_n + \frac{h^*}{2}, \omega_n + \frac{h^*}{2} F(\theta_n, \omega_n)\right) \tag{7}$$

Here h^* refers to the step size and $\theta_n = \theta_0 + nh^*$. The verifiable methodology of the mid-point technique procedure is explained as $\omega_{n+1} = \omega_n + h^* F\left(\theta_n + \frac{h^*}{2}, \omega_n + \frac{1}{2}(\omega_n, \omega_{n+1})\right), n = 0,1,2....$ (8)

The local error at each progression of the mid-point method is of $o(h^{*3})$ and the global error is of the order $o(h^{*2})$. With more computational concentrated, the mid-point calculation error decreases all the more quickly as $h^* \to 0$ and will be a more steady arrangement. The absolute error convergence of this technique is upto 10^{-6}.

4. VALIDATION OF THE RESULTS:

A correlation of mathematical estimations of $f'(0), -g'(0)$ and $\chi'(0)$ is presented for restricting defense that is without unsteady parameter, porosity parameter, stretching parameter, magnetic field, Biot numbers, dimensionless Brownian parameter , reduced thermophoresis parameter, Lewis Number, and suction injection parameter. The correlations of mathematical outcomes to that of Bachok et al. [17] and Turkyilmazoglu [18] have been organized in Table 1. This table affirms us a lawfulness of our mathematical arrangement code for tackling the stream arrangement of the article.

Table 1: A Assessment Of The Values Of $f'(0), -g'(0)$ And $\chi'(0)$ On Fixed Prandtl Number Pr = 6.2 With The Results Of Bachok Et Al. [17] And Turkyilmazoglu [18]

	Bachok et al. [17]	Turkyilmazoglu [18]	Present study
$f'(0)$	0.5102	0.51023262	0.510182515
$-g'(0)$	0.6159	0.61592201	0.615891542
$\chi'(0)$	0.9337	0.93387794	0.933701298

5. DISCUSSION ON THE FINDINGS:

In the current examination, our point is to decipher the attributes of nanofluid stream over pivoting and extending disk and the physical behavior of the mass and thermal transport. To depict the thermal and mass exchange regarding different physical included boundaries, results are staged in figures 2-13. The variety of included physical dimensionless boundaries in the above arrangement of ordinary differential equations that are unsteady parameter S_{utd}, magnetic field parameter M , porosity parameter K, Brownian motion parameter N_B, thermophoresis parameter N_t, Prandtl number Pr, Lewis number Le, stretching parameter s, suction/injection parameter λ, thermal Biot number Bi_t and nanoparticle mass Biot number Bi_c for temperature and concentration conveyances are examined.

Volume 36 No. 2 2023,
ISSN: 1311-1728 (printed version); ISSN: 1314-8060 (on-line version)

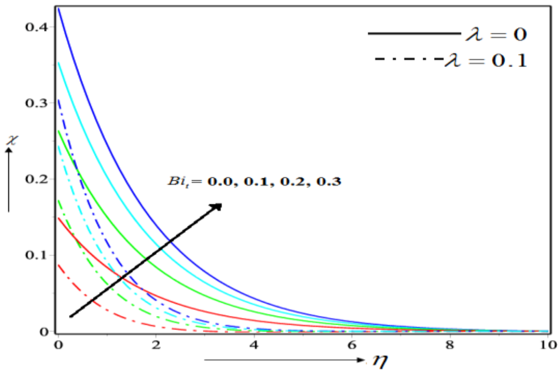

FIGURE 2: TEMPERATURE PROFILE UNDER THE INFLUENCE OF Bi_t

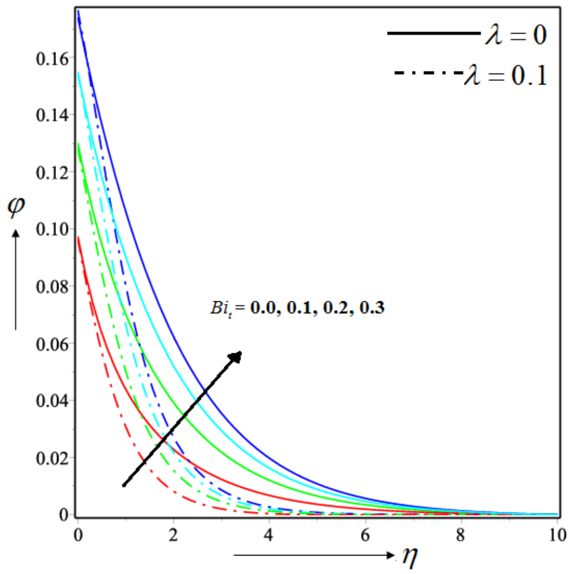

FIGURE 3: NANOPARTICLE CONCENTRATION PROFILE UNDER THE INFLUENCE OF Bi_t

For this, we considered different physical parameters to represent physical structure are $S_{utd} = 1.0,\ M = 0.5,\ K = 0.6,\ N_B = 0.2,\ N_t = 0.3$ and $Le = 1.5$ except if in any case referenced. It ought to likewise be referenced that all plots are moving toward asymptotically the far-field limit conditions.

5.1. INFLUENCE OF THERMAL BIOT NUMBER (Bi_t):

The influences of Bi_t on the heat and mass transfer of the MHD nanofluid flow flowing over rotating and expanding disk have been illustrated in figures 2-4.

ISSN: 1311-1728 (printed version); ISSN: 1314-8060 (on-line version)

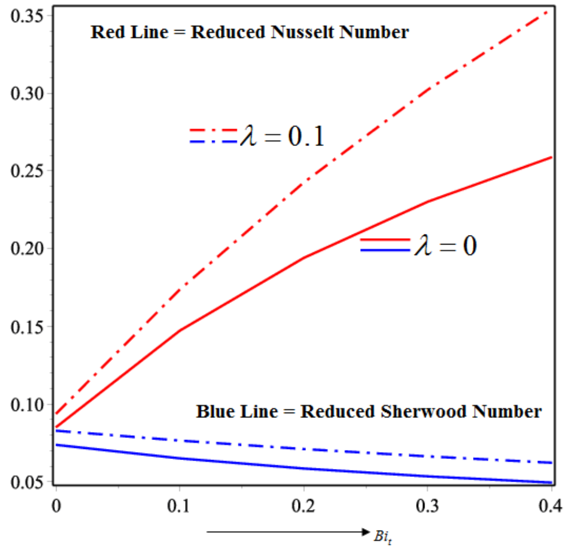

FIGURE 4: HEAT AND MASS TRANSFER PROFILE UNDER THE INFLUENCE OF Bi_t

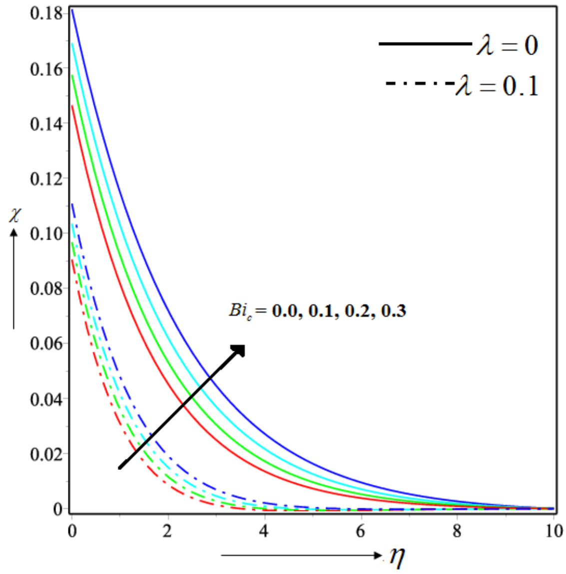

FIGURE 5: TEMPERATURE PROFILE UNDER THE INFLUENCE OF Bi_c

We analyzed our results with and without presence of injection in the flow system. In figure 2 we observe that the thermal profile of the flow is very much influenced by Bi_t. Increasing Bi_t signifies increased heat flow results the elevated thermal profile in the system. Also presence of injection decreases the temperature of the flow. But the presence of thermal Biot number does not affect the difference on the temperature of the flow significantly. Similarly the influence of Bi_t on the nanoparticle mass concentration is shown in figure 3. We observe that influenced heat transfer rate at the disk, intensifies the concentration in the flow.

International Journal of Applied Mathematics
Volume 36 No. 2 2023,
ISSN: 1311-1728 (printed version); ISSN: 1314-8060 (on-line version)

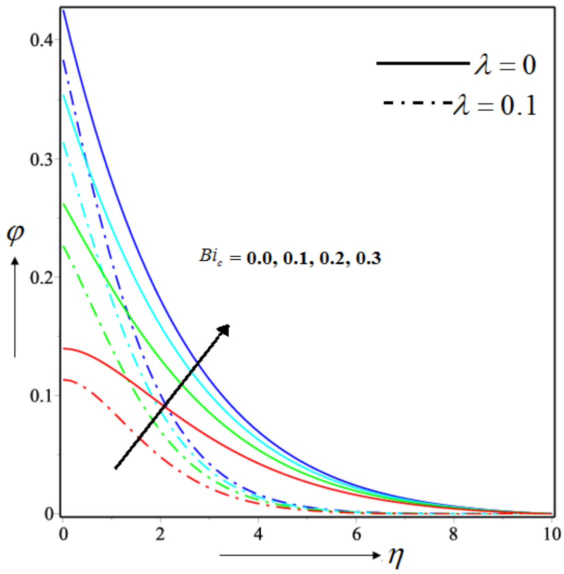

FIGURE 6: NANOPARTICLE CONCENTRATION PROFILE UNDER THE INFLUENCE OF Bi_c

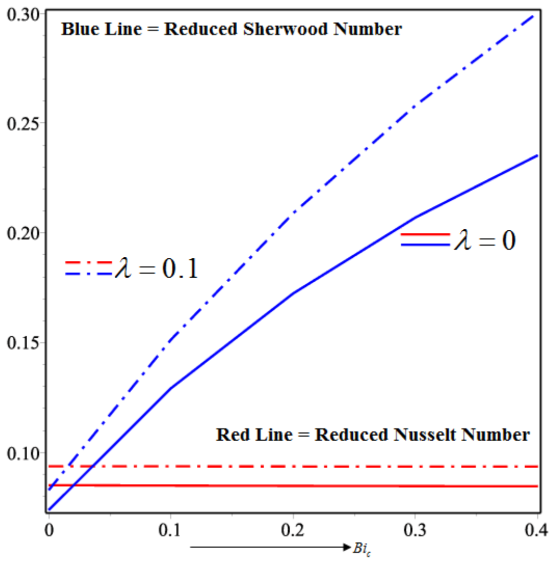

FIGURE 7: HEAT AND MASS TRANSFER PROFILE UNDER THE INFLUENCE OF Bi_c

But presence of injection in the porous disk lessens the nanoparticle volume profile of the flow. In figure 4, we witness that increased Bi_t elevates the ability to heat flow of the system significantly. But it decreases the mass transfer capacity of the flow at the surface.

5.2. INFLUENCE OF NANOPARTICLE MASS BIOT NUMBER (Bi_c):

Temporal profile of the flow seems to be elevated with the rises in mass Biot number in figure 5. The presence of injection lessens the temporal profile of the flow. Here the difference is quite distinctive. Also the presence of injection in the flow diminishes the effectiveness of mass Biot number in the flow. Similar trend is observed in figure 6. Also we witness the effect of Bi_c

Volume 36 No. 2 2023,
ISSN: 1311-1728 (printed version); ISSN: 1314-8060 (on-line version)

is relevant at a distance from the disk. In figure 7, the effect of Bi_c is elevated on mass transfer ability of the flow and consistently increasing. But it does not affect much the heat transfer phenomena of the flow.

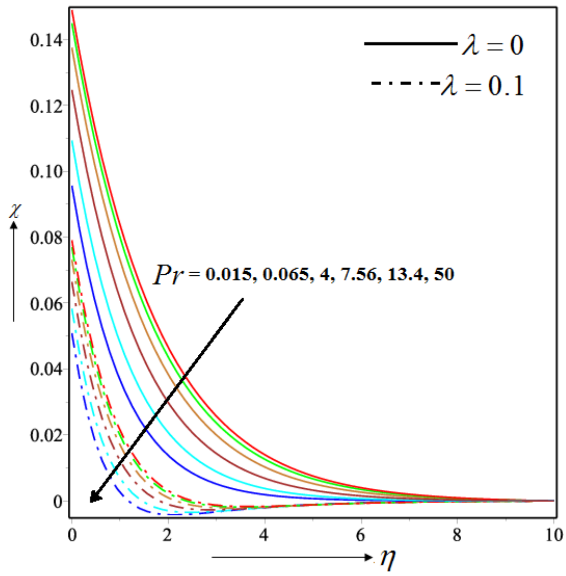

FIGURE 8: TEMPERATURE PROFILE UNDER THE INFLUENCE OF Pr

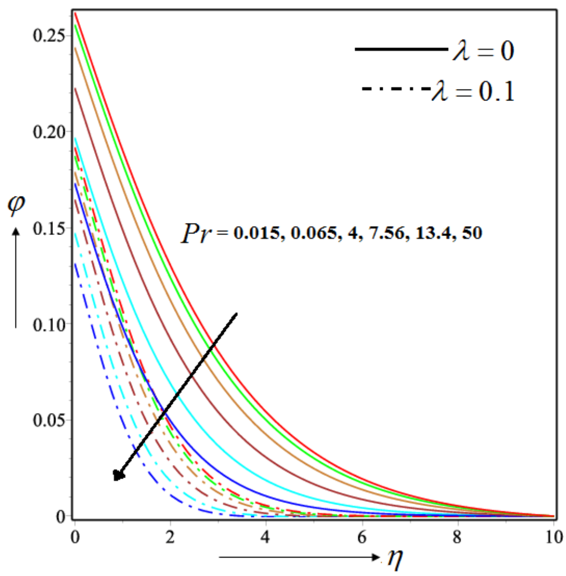

FIGURE 9: NANOPARTICLE CONCENTRATION PROFILE UNDER THE INFLUENCE OF Pr

5.3. INFLUENCE OF PRANDTL NUMBER (Pr):

Figure 8 evidenced that higher Prandtl number diminishes the temperature of the flow system. Prandtl number is a non-dimensional amount that connects the liquid's consistency with the warm conductivity. It subsequently portrays the connection between warm vehicle and energy transport capacity of the nanofluid. Liquids having little Prandtl numbers are honored to have high warm conductivity and in this manner temperature is diminished for higher Prandtl numbers. Additionally joining of infusion in the stream diminishes the transient profile of the stream. Similarly, nanoparticle seems to be on the declined side with increasing in Pr. But in figure 10 we observed that nanofluids with larger higher Pr have higher capacity to flow thermal energy and mass. It is interesting to see that the ability of flow heat and mass is raised significantly within the range of 0-20 of Pr.

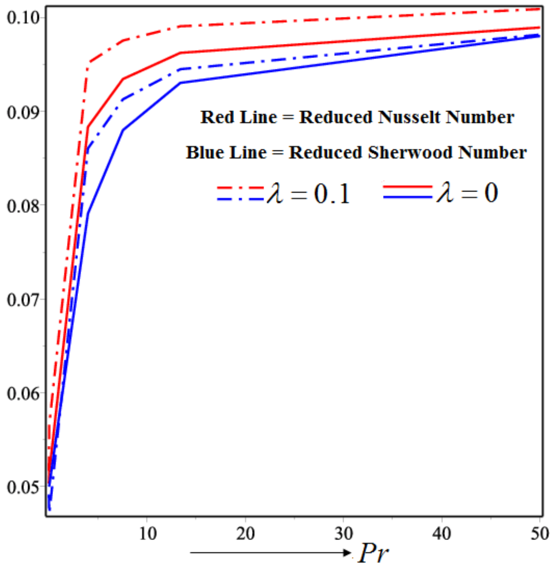

FIGURE 10: HEAT AND MASS TRANSFER PROFILE UNDER THE INFLUENCE OF Pr

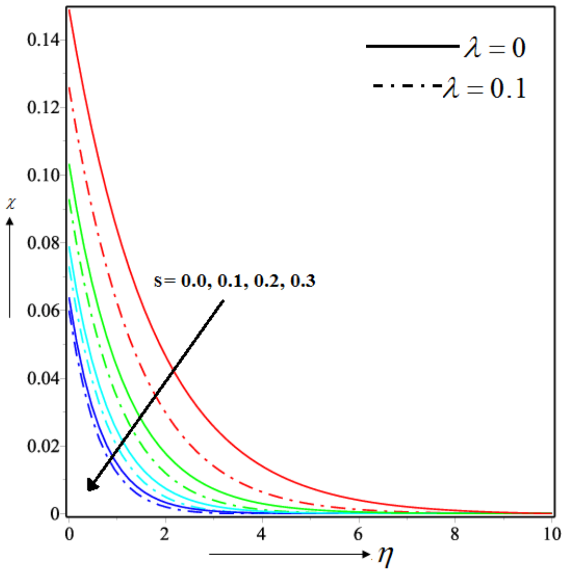

FIGURE 11: TEMPERATURE PROFILE UNDER THE INFLUENCE OF s

5.4. INFLUENCE OF EXTENDING PARAMETER (s):

The extending parameter (s) acts on the boundary of the flow, where $s=0$ means no expansion and $s>0$ means the disk is expending. It has very significant importance on the physical output of the flow system. The temperature of the flow increases with higher s as illustrated in figure 11 since extending disk means higher surface area of the disk. So the fluid gets more area of

ISSN: 1311-1728 (printed version); ISSN: 1314-8060 (on-line version)

contact with the flow surface to absorb thermal energy from the disk and elevate the temporal profile of the flow. But flow with injection shows lower thermal profile than the flow with no injection. In figure 12, the nanoparticle mass density has the similar trend to increased extension of the disk. But the influence of s on both flows with injection and no injection seems to be elevated with higher expansion of the disk. At last in figure we witness that higher expansion of the disk definitely increases the heat and mass flow of the system at the disk but the difference of the outcome gradually vanishes with higher expansion of the disk.

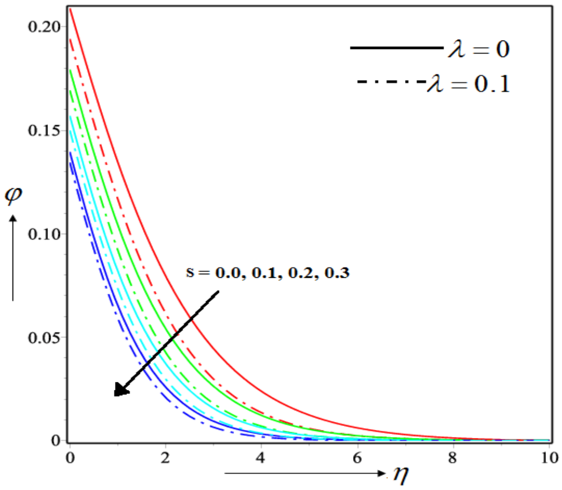

FIGURE 12: NANOPARTICLE CONCENTRATION PROFILE UNDER THE INFLUENCE OF s

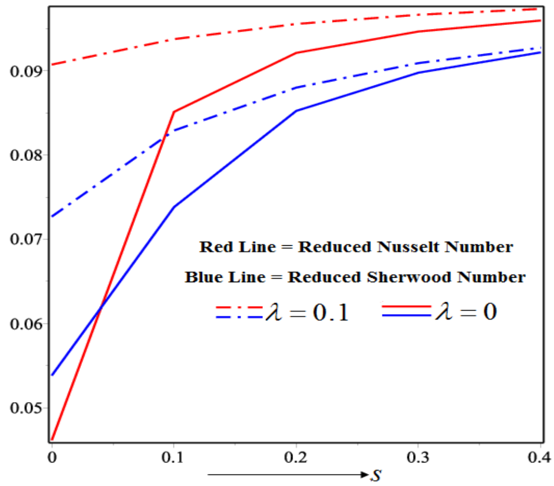

FIGURE 13: HEAT AND MASS TRANSFER PROFILE UNDER THE INFLUENCE OF s

6. CONCLUDING REMARKS:

This article describes the MHD boundary layer flow of nanofluid flowing over an expanding and rotating porous disk. We are trying to look upon the influence of Biot numbers on thermal and mass concentration, Prandtl number and the extending factor on the properties of the flow under the flows with injection and on injection conditions. The results are staged in proper graphs above and we discussed the results of our investigation above. Now here we highlight the notable outcomes in a nutshell.

A. Thermal and mass density Biot numbers elevate the thermal and mass density profile of the flow with the presence of injection in the flow.

B. Thermal Biot number elevates the ability of heat flow in the system and mass density Biot number intensifies mass transfer capability of the flow remarkably.

C. Presence of infusion in the stream consistently raises the warmth and mass exchange execution of the stream framework.

D. Fluid with higher Prandtl number diminishes both temperature and mass concentration of the flow but it intensifies heat and mass transfer ability of the flow significantly.

E. Similarly, extending disk lessens the temperature and mass density of the flow but enlarge the heat and mass transfer rate of the flow system.

REFERENCES:

[1] Choi SU, Eastman JA. Enhancing thermal conductivity of fluids with nanoparticles. Argonne National Lab., IL (United States); 1995 Oct 1.

[2] Buongiorno J, Convective transport in nanofluids, ASME Journal of Heat Transfer, 2006; 128: 240–250 .

[3] Hayat T, Muhammad T, Alsaedi A, Alhuthali MS. Magnetohydrodynamic three-dimensional flow of viscoelastic nanofluid in the presence of nonlinear thermal radiation. Journal of Magnetism and Magnetic Materials. 2015;385:222-9.

[4] I. V. Shevchuk, Modelling of convective heat and mass transfer in rotating flows, Springer; 2016, DOI:10.1007/978-3-319-20961-6

[5] Von Karman T. Uber laminare und turbulente reibung. Z Angew Math Mech. 1921;1:233–52.

[6] Millsaps K, Pohlhausen K. Heat transfer by laminar flow from a rotating plate. Journal of the Aeronautical Sciences. 1952;19(2):120-6.

[7] Stuart JT. On the effects of uniform suction on the steady flow due to a rotating disk. The Quarterly Journal of Mechanics and Applied Mathematics. 1954;7(4):446-57..

[8] Riley N. The heat transfer from a rotating disk. The Quarterly Journal of Mechanics and Applied Mathematics. 1964 Aug 1;17(3):331-49.

[9] Benton ER. On the flow due to a rotating disk. Journal of Fluid Mechanics. 1966 Apr;24(4):781-800.

[10] Kuiken HK. The effect of normal blowing on the flow near a rotating disk of infinite extent. Journal of Fluid Mechanics. 1971 Jun;47(4):789-98.

[11] Watson LT, Wang CY. Deceleration of a rotating disk in a viscous fluid. The Physics of Fluids. 1979 Dec;22(12):2267-9.

[12] Fang T, Tao H. Unsteady viscous flow over a rotating stretchable disk with deceleration. Communications in Nonlinear Science and Numerical Simulation. 2012 Dec 1;17(12):5064-72.

[13] Türkyılmazoglu M, Uygun N. Basic compressible flow over a rotating disk. Hacettepe Journal of Mathematics and Statistics. 2004;33:1-0.

[14] Miklavčič M, Wang CY. The flow due to a rough rotating disk. Zeitschrift für angewandte Mathematik und Physik ZAMP. 2004 Mar 1;55(2):235-46.

[15] Turkyilmazoglu M. The MHD boundary layer flow due to a rough rotating disk. Z Angew Math Mech. 2010;90:72–82.

[16] Turkyilmazoglu M. MHD fluid flow and heat transfer due to a stretching rotating disk. International Journal of Thermal Sciences. 2012 Jan 1;51:195-201.

[17] Bachok N, Ishak A, Pop I. Flow and heat transfer over a rotating porous disk in a nanofluid. Physica B: Condensed Matter. 2011 Apr 15;406(9):1767-72.

[18] Turkyilmazoglu M. Nanofluid flow and heat transfer due to a rotating disk. Computers & Fluids. 2014 May 1;94:139-46.

[19] Doh DH, Muthtamilselvan M. Thermophoretic particle deposition on magnetohydrodynamic flow of micropolar fluid due to a rotating disk. International Journal of Mechanical Sciences. 2017 Sep 1;130:350-9.

[20] Tabassum M, Mustafa M. A numerical treatment for partial slip flow and heat transfer of non-Newtonian Reiner-Rivlin fluid due to rotating disk. International Journal of Heat and Mass Transfer. 2018 Aug 1;123:979-87.

[21] Appelquist E, Schlatter P, Alfredsson PH, Lingwood RJ. Turbulence in the rotating-disk boundary layer investigated through direct numerical simulations. European Journal of Mechanics-B/Fluids. 2018 Jul 1;70:6-18.

[22] Wen D, Ding Y. Formulation of nanofluids for natural convective heat transfer applications. International Journal of Heat and Fluid Flow. 2005 Dec 1;26(6):855-64.

[23] Liao Z, Poh CK, Huang Z, Hardy PA, Clark WR, Gao D. A numerical and experimental study of mass transfer in the artificial kidney. J. Biomech. Eng.. 2003 Aug 1;125(4):472-80.

[24] Kooijman HA, Taylor R. Modelling mass transfer in multicomponent distillation. The Chemical Engineering Journal and the Biochemical Engineering Journal. 1995 Apr 1;57(2):177-88.

[25] Saif RS, Hayat T, Ellahi R, Muhammad T, Alsaedi A. Darcy–Forchheimer flow of nanofluid due to a curved stretching surface. International Journal of Numerical Methods for Heat & Fluid Flow. 2019 Jan 7.

[26] Mehmood Z, Iqbal Z, Azhar E, Maraj EN. Nanofluidic transport over a curved surface with viscous dissipation and convective mass flux. Zeitschrift für Naturforschung A. 2017 Mar 1;72(3):223-9.

[27] Hayat T, Aziz A, Muhammad T, Alsaedi A. Numerical study for nanofluid flow due to a nonlinear curved stretching surface with convective heat and mass conditions. Results in physics. 2017 Jan 1;7:3100-6.

[28] Imtiaz M, Hayat T, Alsaedi A. MHD convective flow of Jeffrey fluid due to a curved stretching surface with homogeneous-heterogeneous reactions. Plos one. 2016 Sep 1;11(9):e0161641.

ISSN: 1311-1728 (printed version); ISSN: 1314-8060 (on-line version)

[29] Acharya N, Das K, Kundu PK. Outlining the impact of second-order slip and multiple convective condition on nanofluid flow: a new statistical layout. Canadian Journal of Physics. 2018;96(1):104-11.

[30] Chakraborty T, Das K, Kundu PK. Multiple convection-driven Falkner-Skan flow of Carreau nanofluid along a permeable wedge: An analytical approach. Heat Transfer—Asian Research. 2019 May;48(3):914-37.